www.amlett.com, www.vbripress.com/aml, DOI: 10.5185/amlett.2015.5921 Published online by the VBRI Press in 2015

Swift heavy ion induced functionality in nanocrystalline CdS thin films: Role of growth temperature

Pragati Kumar[1*], Nupur Saxena[1], Avinash Agarwal[2], Vinay Gupta[1]

[1]*Department of Physics & Astrophysics, University of Delhi, Delhi 110 007, India*
[2]*Department of Physics, Bareilly College, Bareilly 243 005 (U. P.), India*

[*]Corresponding author. Tel.: (+91) 11-27667036; E-mail: pkumar.phy@gmail.com

Received: 03 March 2015, Revised: 30 May 2015 and Accepted: 08 June 2015

ABSTRACT

Influence of growth temperature on swift heavy ion (SHI) induced structural and optical functionality in CdS thin films is explored for photonic applications. Intense green emission is observed in nanocrystalline CdS thin films grown by pulsed laser deposition (PLD) at two different substrate temperatures (T_s): room temperature (RT) and 200 ºC. The role of T_s and its implications on the effect of dense electronic excitation provoked by swift heavy ion irradiation (SHII) on various optical and structural properties of CdS films is investigated under the influence of 70 MeV $^{58}Ni^{+6}$ ion beam. It reveals from the present studies that T_s may crucially affect the crystalline structure, vibrational and electronic states of the film and thereafter the functionality induced by ion beam. It is found that ion beam is capable to transform structural phase from mixed phase of cubic and hexagonal structure to either pure cubic or pure hexagonal phase of CdS depending upon the pre-existing preferred orientation in pristine film. The modification in crystallite size and band gap due to impact of ion beam is found to be strongly dependent on pre-existing structural phase, as determined by T_s. The studies presented here confirm that initial growth conditions play a key role even after post deposition SHII treatment in selecting precisely the functional behavior of the films.

Keywords: Nanocrystalline CdS thin films; pulsed laser deposition; ion beam irradiation; photoluminescence.

Introduction

Thin films of wide bandgap II-VI semiconductors are receiving widespread attention for numerous applications because they exhibit emission in visible region of electromagnetic spectrum. Particularly, CdS thin films concerned superfluous attention as their bandgap emission (~2.42 eV for bulk) is expected to lie in the proximity of the highest sensitivity of the human eye, i.e., green light. Thin films of CdS nanoparticles (NPs) have wide applications in photonic devices like lasers [**1, 2**], light emitting diodes (LEDs) [**3, 4**], electrochemiluminescence sensor [**5**], gas sensors [**6**], bio-imaging [**7**] and solar cells [**8,9**] etc because of its appropriate bandgap, imperative optical properties, admirable stability and straightforward fabrication procedure. Thin film of CdS has been synthesized by various chemical and physical routs and blue, green, yellow, orange and red emissions are observed [**3, 10-15**]. However, a stable source of green emission (GE) is the challenge that limits the performance of many current optoelectronic and photonic devices [**10**]. Among various deposition techniques, pulsed laser deposition (PLD) has been proven as a versatile technique to maintain crystal purity and stoichiometry of film in a cold-wall ambience. Previously, we have obtained almost stable GE from PLD grown CdS (PLDCdS) thin films and studied the effect of thermal annealing **[16]** and ion beam irradiation [**17**] on it. In this article we emphasize on swift heavy ion (SHI) induced functionality in structural and optical properties of PLDCdS thin films and role of T_s to select these functionalities. Since, T_s plays a crucial role to modify various properties like: growth direction of film (direction of c-axis from parallel to perpendicular just by increasing it) [**18**], structural phase change [**19**], growth rate or thickness, grain size, and resistivity [**20, 21**], texture coefficient, defect density [**20**], refractive index [**21**], morphology and emission [**22**]. However, the role of T_s to decide SHI induced functionality in PLDCdS is rarely explored.

Swift heavy ion irradiation (SHII) is a resourceful tool used for material engineering and characterization. A variety of effects in materials including high pressure phase generation [**23**], defect creation [**17, 24-26**], defect annealing, crystallization [**26, 27**], amorphization [**28**], dissolving of nanoparticles [**29**] and nanophase formation [**30**] etc. are possible by SHII. The effect of SHII on various properties of CdS thin films grown by different deposition techniques [**11-13, 17, 25, 26, 31, 32**] has been reported. Though there are few reports on SHI induced enhancement in emission in CdS thin films grown by different techniques [**12, 13, 17, 26**]. Still to the best of our

knowledge, the role of T_s to control the functionality induced by SHII in CdS thin films is unexplored. Recently, we examined the role of SHII in creation/annihilation of defects and variation of defect density as a function of ion irradiation fluence and therefore the shape of emission spectra [**17**]. In present work we are focusing on the role of T_s to select specifically SHII induced functional behavior of the films.

In the present letter, we have explored the effect and selectivity of SHII on structural and luminescence properties of PLDCdS thin films. Here, we demonstrate, SHII is appropriate to produce stable, intense, and broad GE from PLDCdS thin films, which is the demand of current existing photonic devices like fluorescent sensors, green LEDs etc. Furthermore, the role of T_s to activate and control various properties of films by means of SHII has been investigated. The importance of this work is to analyze the growth conditions of PLDCdS thin films in detailed and systematic way and their further impact to enhance its utility in futuristic devices by means of SHII. These studies confirm that the pre-existing conditions play a significant role in ion-solid interaction during SHII and selecting features of final product.

Experimental

Thin film deposition and SHII

The procedure used here for CdS thin films growth by PLD setup is fully described elsewhere [**16, 17**]. All the samples investigated were synthesized by PLD to guide 248 nm emission of an ultraviolet laser source: a pulsed excimer KrF laser onto a target of chemically synthesized CdS quantum dots (QDs). The laser beam of energy 300 mJ/pulse with pulse width of 10 ns and repetition rate 10 Hz was focused onto a rotating target that was kept at a distance of 5.5 cm from substrate (Si, glass and carbon coated Cu TEM grid) and mounted at an oblique angle of 30° with respect to the incident laser beam. The films were deposited at two different T_s: (i) room temperature (RT) and (ii) 200ºC inside a stainless steel vacuum chamber keeping base pressure better than 5×10^{-6} Torr. To examine the ion beam induced functionality in films and role of T_s, thin films so prepared were irradiated at different fluences (ions dose) of 70 MeV Ni^{6+} ions using the 15 UD Pelletron at Inter University Accelerator Centre (IUAC), New Delhi, India. The SHII was performed inside a vacuum chamber (~ 2×10^{-6} Torr) at room temperature. The ion beam of almost constant current of ~ 1 pnA (particle nano Ampere) was scanned over an area of ~ $1cm^2$ of the sample with an electromagnetic scanner to ensure the uniform irradiation. The electronic energy loss, nuclear energy loss, and range of the incident 70 MeV Ni ion in CdS were simulated using stopping and range of ions in matter (SRIM) [**33**], and found to be 10.58 keV/nm, 0.031 keV/nm and 10.94 µm respectively.

Characterizations

For structural studies, glancing angle x-ray diffraction (GAXRD) measurement at an angle of 1° using Bruker D8 diffractometer (Cu K_α radiation, λ = 1.54 Å) and micro-Raman spectroscopy measurement, using Renishaw Invia Raman microscope with excitation wavelength of 514 nm from an Ar-ion laser, were carried out. The microstructure of samples was examined by transmission electron microscopy (TEM) using Tecnai G20-Stwin operating at 200 kV with point resolution of 1.44 Å, line resolution of 2.32 Å, and line-type super twin lenses. To study the optical properties, UV-vis absorption spectroscopy (Hitachi 3300 UV/visible spectrophotometer) was performed on the films deposited on glass substrate and photoluminescence (PL) measurement was carried out at room temperature using Jobin Yvon Triax 550 monochromator combined with a liquid-nitrogen cooled InGaAs detector. A He-Cd laser (wavelength 325 nm) is used as the excitation source.

Results and discussion

The microstructure and surface morphology is studied using TEM micrographs. TEM micrographs of the pristine films grown at T_s= RT and 200ºC followed by irradiation at 1×10^{13} ions/cm^2 fluence are shown in **Fig. 1a** and **1c** and **Fig. 1b** and **1d** respectively and inset shows the lognormal fitting in corresponding size distributions. It is found that the standard deviation is varied for pristine to irradiated film from 0.14 to 1.0 & 0.12 to 0.27 for the films grown at T_s=RT & 200ºC respectively. TEM analysis shows that for RT grown film, average particle size increases from ~ 8.2 nm to 10.7 nm (around 30%) and average size reduces from ~ 9.2 nm to 4.8 nm (around 48%) for the film grown at 200 ºC to film irradiated at a fluence of 1×10^{13} ions/cm^2, respectively.

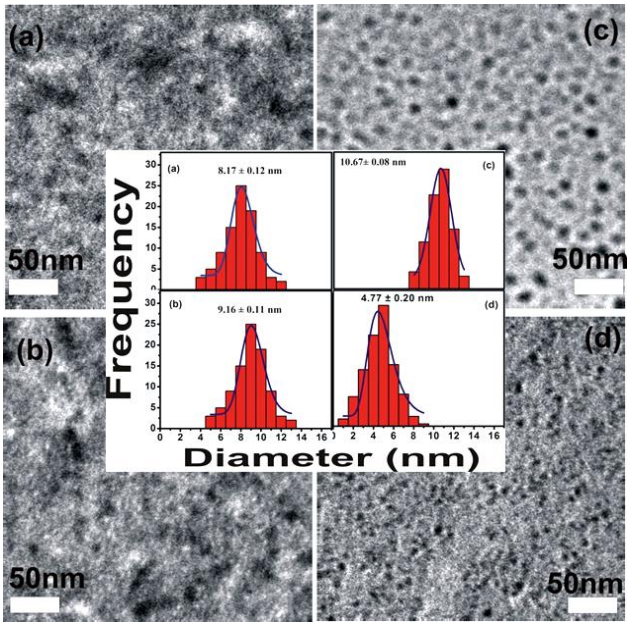

Fig. 1. TEM micrograph of CdS (a) & (c) pristine films and (b) & (d) irradiated at 1×10^{13} ions/cm^2 films and grown at RT & 200 ºC respectively. Inset particle size distributions (solid curve represents lognormal distribution).

To investigate the effect of SHII on the film's structure and its associated properties, GAXRD scan is carried out. GAXRD scan of films deposited at two different T_s (i) RT and (ii) 200ºC and further irradiated at different fluences are shown in **Fig. 2a** and **2b** respectively. From **Fig. 2a**, it is clear that pristine film deposited at RT is in mixed phase of cubic (zincblende) and hexagonal (wurtzite) structure as

cleared from the appearance of the diffraction peaks at 24.87°, 26.60°, and 28.1° corresponding to planes (100), (002), and (101) respectively of wurtzite (WZ) structure (PCPDFWIN –800006) and peaks at 43.9° and 52° corresponding to planes (220) and (311) respectively of zincblende (ZB) structure (PCPDFWIN –751546).

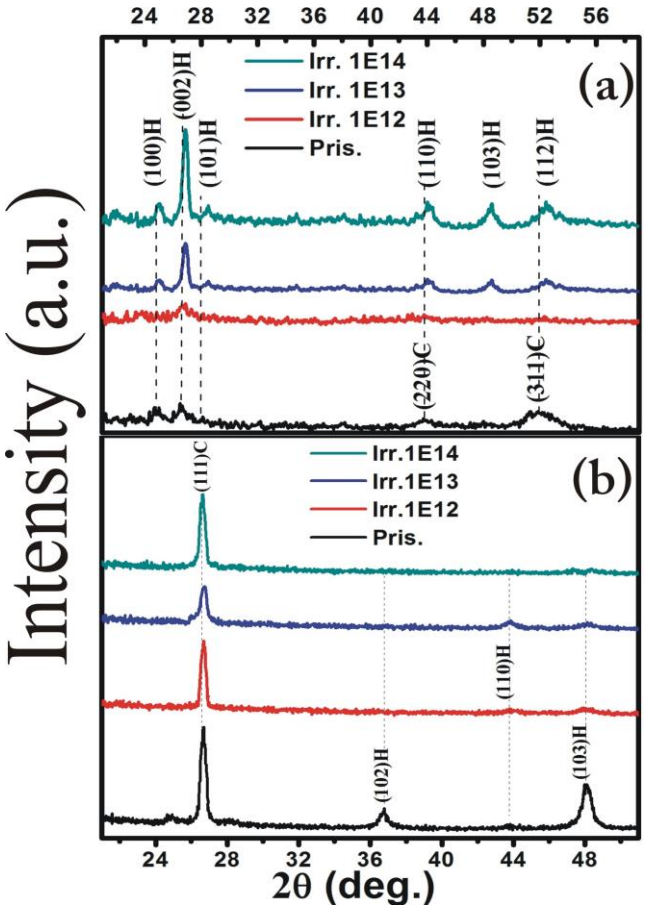

Fig. 2. GAXRD patterns of CdS thin films irradiated at different fluences and grown at (a) RT (b) 200 ºC.

It is observed that the intensity of all the diffraction peaks increases with increase in ion fluence and WZ phase of CdS starts dominating at irradiation fluence of 1×10^{12} ions/cm^2 as confirmed by the appearance of diffraction peaks at ~ 48.2º corresponding to (103) plane (PCPDFWIN − 010783) of WZ phase. It can be seen that a clean hexagonal phase is developed at irradiation fluence 1×10^{13} ions/cm^2. Increase in intensity and sharpness of diffraction peaks after irradiation reveals enhancement in crystallinity and thereby crystallite size induced by SHII. It has been ascribed to defect annealing by various groups [**13, 34**]. SHII provokes shift in all diffraction peaks towards higher diffraction angle than that in pristine film. Here we observed compressive stress induced by SHII as the peaks are shifted towards higher diffraction angle as compared to pristine film as well as bulk powder data. The position of prominent peak correspond to plane (022) becomes 26.70º, 26.80º, and 26.88º for the films irradiated at fluence 1×10^{12} ions/cm^2, 1×10^{13} ions/cm^2, and 1×10^{14} ions/cm^2 respectively.

The different orientation of mixed WZ and ZB phase is illustrated by pristine film grown at T_s= 200°C as shown in **Fig. 2 b.** The diffraction peak at 26.64° is assigned to (111) plane of ZB structure whereas the peaks at 36.8° and 48.1° are assigned to planes (102) and (103) respectively of WZ structure (PCPDFWIN − 020549). It is clearly seen from **Fig. 2 b** that there is significant reduction in peak intensity of plane (111) and small increase in FWHM for films irradiated with fluence of 1×10^{12} ions/cm^2 and 1×10^{13} ions/cm^2 which results due to reduction of crystallinity and particle size. The existing literature suggests that it might be related to the formation of point defects, defect clusters, or creation of additional grain boundaries **[13, 17, 24, 26]** due to SHII. Besides, very small compressive stress is observed for the pristine film as manifested from the shift of (111) peak by an amount of 0.1º towards higher diffraction angle from its corresponding value for bulk (2θ = 26.55º; PCPDFWIN − 750581). It may be ascribed to residual stress generated in film during deposition or due to the lattice mismatch between the film and substrate [**25**]. SHI induced enhancement in the compressive stress for films irradiated at a fluence of 1×10^{12} ions/cm^2 and 1×10^{13} ions/cm^2 is observed as evident from positions (i.e. 2θ ≈ 26.68º and 26.73º) of diffraction plane (111). Additionally, at same irradiation fluence a new diffraction peak at an angle 2θ ≈ 43.77º corresponding to plane (110) is emerged. On further increasing the fluence, peak intensity is increased considerably with small shift in peak position towards lower diffraction angle. The increase in peak intensity indicates improvement in crystallinity and crystallite size.

It is significant to highlight here that the film irradiated at a fluence of 1×10^{14} ions/cm^2 illustrates structural phase transition from mixed phase to cubic phase as pointed out by vanishing of crystalline planes (110) and (103). Such a structural phase transition has been reported by Chi et al. [**35**] for CdS pellets under grinding and hydraulic pressure and previously by our group for PLDCdS films after post deposition treatments like annealing **[16]** and SHII [**17**]. It may be attributed to reshuffling of atoms caused by SHI induced dense electronic excitations that leads to excessively high temperature and pressure in the ion zone. This is consistent with the report by Ghosh et al. [**36**] about the WZ crystal structure of uncapped CdS nanoparticles. They found that WZ phase is extremely unstable and undergoes transformation towards ZB phase under all thermodynamic conditions like pressure, growth temperature, time etc. They predict that the rate of transformation is higher under high pressure at room temperature as compared to other thermodynamic conditions and explained it on account of the total energy of the system calculated by ab-initio method.

It has been reported that shift in peak position is a consequence of the modification of lattice strain and annihilation/creation of diffraction peaks may be related to disorientation/specific preferential orientation during recrystallization induced by SHII. Since, SHI induced dense electronic excitation can result in a momentary growth of the lattice temperature to very high value this leads to large amplitude oscillations in the lattice and a bond splitting phenomena linked with atomic displacements followed by certain collective atomic reorganizations takes place [**37**]. Singh et al. [**38**] studied dose dependent (fluence dependent) shifting in diffraction peak for PLD

grown textured ZnO thin films and reported that shifting in peak position possibly arises due to lattice strain modification after ion beam irradiation. Since, the magnetic, electrical and optical properties of film may be modified largely due to so produced strain or stress in the films therefore, it is fruitful to study the role of T_s in generation of strain or stress in the films due to SHII. For this purpose, the stress (σ) has been calculated using the relation [**39, 40**]:

$$\sigma(\text{GPa}) = -\frac{E}{2\upsilon}\frac{(\text{lattice parameter}_{\text{Film}} - \text{lattice parameter}_{\text{Bulk}})}{\text{lattice parameter}_{\text{Bulk}}}$$

where, E=bulk modulus, υ= Poisson's ratio having values 62.7 GPa and 0.37 respectively for CdS [**41**]. The lattice parameters used for RT grown film is 6.682 Aº (PCPDFWIN –800006) and for film grown at 200ºC is 5.81Aº (PCPDFWIN – 750581). **Fig. 3** shows the variation of stress and area contributed by preferred phase in the films with ion irradiation fluence. It can be clearly seen that the contribution of preferred phase (WZ) and SHI induced stress increases with increase in ion fluence for the films grown at RT. Whereas, for the films grown at 200ºC the contribution of preferred phase (ZB) decreases with increase in ion fluence upto 1×10^{13} ions/cm^2 and stress increases. At the highest fluence contribution of ZB phase increases in the film and stress decreases.

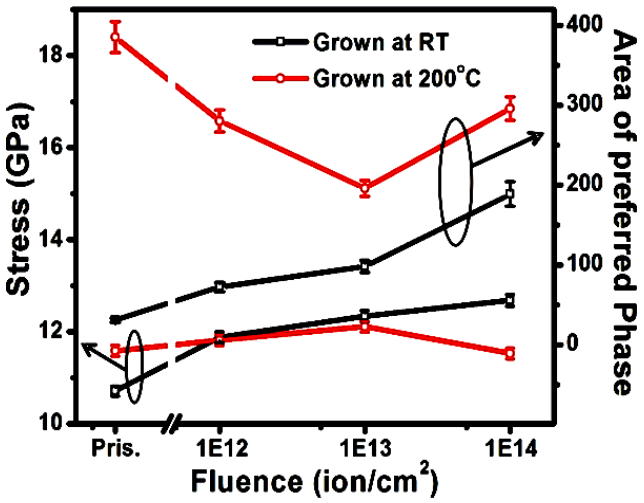

Fig. 3. Dose dependent variation in stress and area of preferred phase in CdS thin films grown at different T_s.

The underlying mechanism for different orientations of mixed phase observed in the pristine films deposited at two different T_s's may be as follows: T_s is one of the main thermodynamic parameters that decides the growth mechanism. The surface mobility of the adatom (vapor atoms) plays a crucial role for the crystallinity of film. Usually, the adatom will diffuse through several atomic distances to acquire a stable location within the newly formed film. The adatom's surface diffusivity is determined by surface temperature of the substrate. The rapid and defect free crystal can be grown at high temperature. Whereas, energetic particle impingement may overwhelm the low temperature crystal growth and results in disordered or even amorphous structures. Here, we observe that the crystallinity of pristine film grown at 200°C is better than that grown at RT.

The behavior shown by stress and contribution of preferred phase with ion fluence may be because of the orientation (111) of substrate. During SHII, recrystallization is taking place in the films and the films are orienting according to their pre-existing phase. Moreover, as the contributed area of WZ phase for the film grown at RT increases with increase in ion fluence, it results in an increase in lattice mismatch between substrate and film, consequently stress increases in the films. Similarly for the films grown at 200 ºC, contributed area of ZB phase reduces (i.e. contributed area of WZ phase increases) and illustrates same result in stress variation upto fluence 1×10^{13} ions/cm^2. On the other hand at fluence 1×10^{14} ions/cm^2 due to increase in contribution of ZB phase lattice mismatch reduces and hence the stress. Therefore, it may be concluded that developed stress as a consequence of SHII also depends on pre-existing structural phase of the films.

In micro Raman study, five optical vibrational Raman active modes at ~ 302 cm^{-1}, 390 cm^{-1}, 603 cm^{-1}, 690 cm^{-1}, and 903 cm^{-1} are observed in all samples (**Fig. S$_1$a** and **S$_1$b** are given in supporting information).

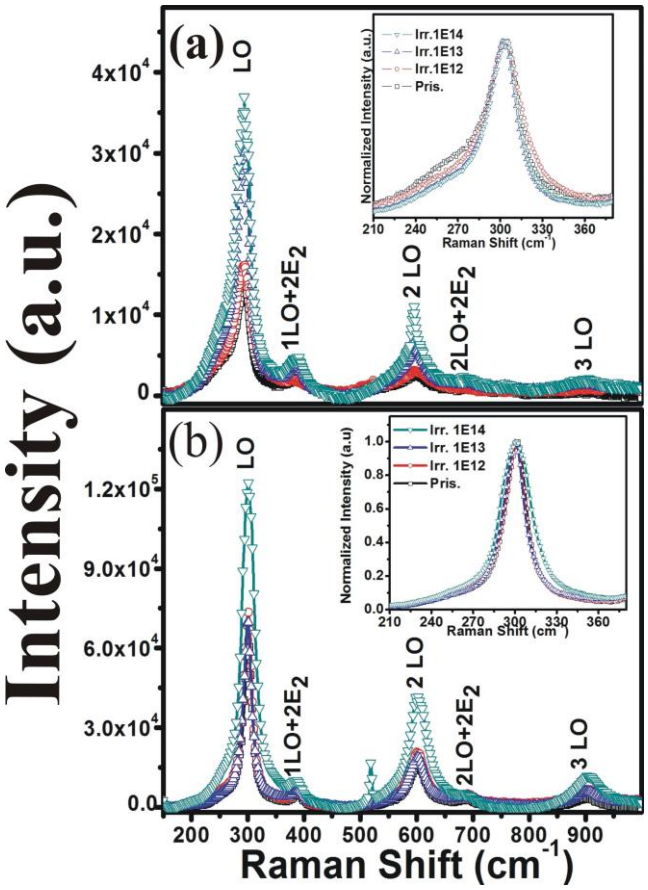

Fig. S$_1$. Raman spectra of CdS thin films irradiated at different fluences and grown at (a) RT (b) 200 ºC. (Inset) Normalized intensity Vs Raman shift of LO mode.

The intense and broad peaks at ~ 302 cm^{-1}, 603 cm^{-1}, and 903 cm^{-1} are assigned to fundamental optical phonon mode (LO), the first over tone mode (2LO) and the second overtone mode (3LO) of CdS. The weak Raman peaks at ~

390 cm^{-1} and 690 cm^{-1} result from multiphonon scattering and identified as those corresponding to the vibrational modes LO+2E_2 and 2LO+2E_2 respectively [**16, 17**]. One can easily see SHI induced enhancement in intensities of LO, 2LO, and 3LO modes from **Fig. S1a** and reduction in asymmetry of LO mode (Inset Fig.S_1a) continuously up to highest fluence for RT grown films. Whereas, the behavior of intensity and asymmetry variation of LO mode with ion fluence is quite different for the film grown at T_s = 200 ºC as evident from **Fig. S_1b**. It is observed that frequency of LO mode shifts by ~ 0.50 cm^{-1}, 2.0 cm^{-1}, and 1.0 cm^{-1} towards lower frequency side compared to that of its corresponding pristine film after exposing the samples to fluence 1×10^{12} ions/cm^2, 1×10^{13} ions/cm^2, and 1×10^{14} ions/cm^2 respectively.

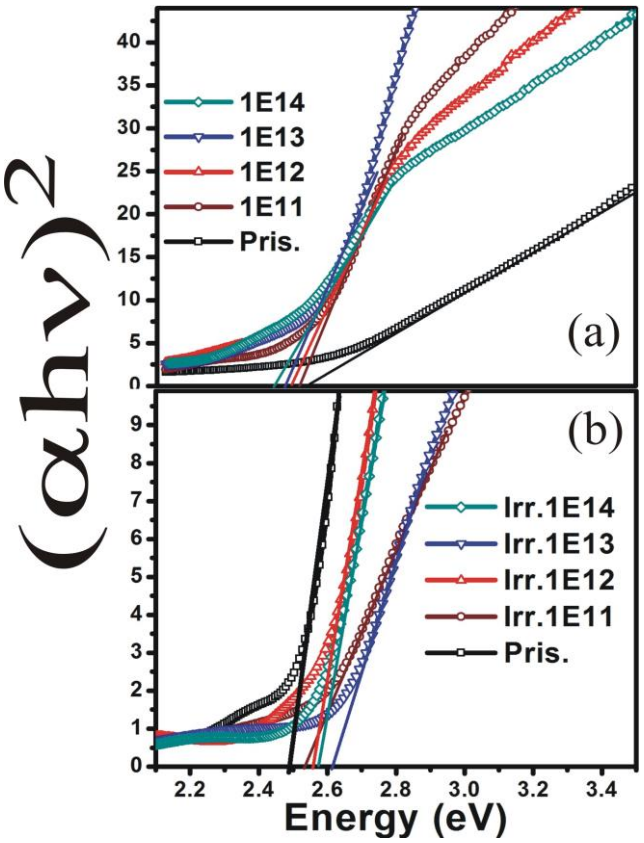

Fig. 4. Tauc plot of CdS thin films irradiated at different fluences and grown at (a) RT (b) 200ºC.

Generally the asymmetry and shifting in peak position is a consequence of quantum confinement effect. For RT grown films reduction in asymmetry may be resulted from increase in particle size. Here the reduction in asymmetry of LO mode indicates SHI induced grain growth which is in support of GAXRD results. The shifting of peak for films grown at 200 ºC may be attributed to phonon localization by high density of lattice defects [**42**] and/or structural strain induced grain fragmentation [**17, 26**] due to energetic heavy ions. The difference in intensities of Raman modes for the pristine films grown at two different T_s is due to the difference in crystallinity of films at their respective T_s.

UV-Visible absorption spectra are recorded for the films deposited on glass substrates to study the SHII effect on energy band gap of CdS thin films. **Fig. 4a** and **4b** shows Tauc plots of the films grown at two different T_s and irradiated at different fluences. A continuous reduction in bandgap after SHII up to fluence 1×10^{14} ions/cm^2 is observed for RT grown films (**Fig. 4a**). Whereas, the film grown at T_s = 200 ºC show SHI induced enhancement in band gap upto irradiation fluence 1×10^{13} ions/cm^2 and then reduction at higher irradiation fluence (**Fig. 4b**).

The direct band gap values are estimated by extrapolating the linear fit to the energy axis from the plot of $(\alpha h\nu)^2$ versus energy. The estimated values are ~ 2.53 eV, 2.52 eV, 2.49 eV, 2.48 eV, and 2.44 eV for RT grown films and ~ 2.46 eV, 2.52eV, 2.55 eV, 2.62 eV, and 2.56 eV for the films grown at 200 ºC, corresponding to pristine, irradiated at 1×10^{11} ions/cm^2, 1×10^{12} ions/cm^2, 1×10^{13} ions/cm^2, and 1×10^{14} ions/cm^2 fluence respectively. It is obvious that the bandgap of pristine film grown at either T_s is blue shifted than the bandgap of bulk CdS (~ 2.42 eV) due to quantum confinement. The large bandgap of pristine film grown at RT than that grown at 200 ºC, again indicates that crystallinity of films grown at 200 ºC is comparatively better. The average particle size is calculated using mass approximation formula for energy shift [**17, 26**]. Dose (fluence) dependent variation of average particle size and strength of electron phonon coupling measured by I_{2LO}/I_{LO} ratio [**16**] is shown in **Fig. 5**.

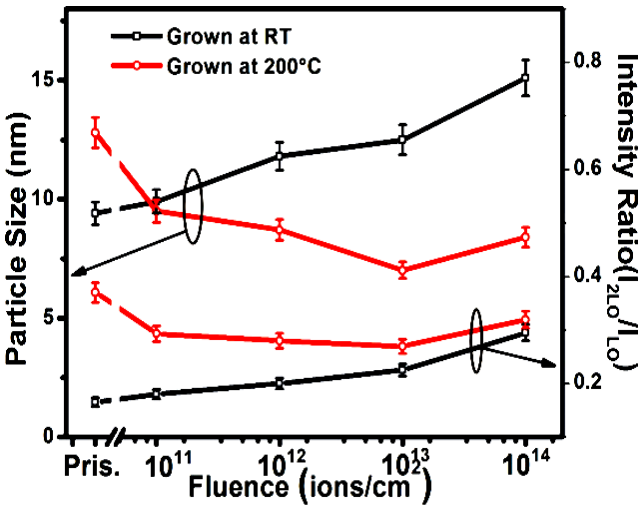

Fig. 5. Dose dependent variation in particle size and intensity ratio (I_{2LO}/I_{LO}) of CdS thin films grown at different T_s.

It can be seen that the behavior of intensities ratio (overtone to its fundamental) and particle size with ion fluence are different for two set of samples. However, for either of the set, the ratio I_{2LO}/I_{LO} varies in accordance to the variation in particle size on changing the dose of ion. Therefore, it may be concluded from the present study that electron-phonon interaction is a function of particle size, irrespective of the structure. It is also illustrated from **Fig. 5** that the particle size is increased by 33% & reduced by 45% for the samples grown at RT & 200 ºC respectively and irradiated with fluence 1×10^{13} ions/cm^2 than that of their respective pristine samples. It follows that the changes in average particle size so estimated from TEM micrographs and UV-Vis measurements are in well agreement. The enhancement/reduction in particle size at different ion irradiation fluences is obvious from observed

rise/fall in intensity of peak corresponds to preferred orientation of planes in GAXRD pattern, shifting of LO peak in Raman spectra, band gap decrease/increase in UV-Vis and particle size enhancement/reduction in TEM micrographs.

SHI induced growth in crystallite size for RT grown films is in accordance to previous reports [**13, 17, 24, 26, 43, 44**]. It may be due to either SHI induced coalescence of particles due to annealing effect produced by ion beam, which results in an increase in the particle size and decrease in the surface-to-volume ratio [**13**] or SHI induced Ostwald ripening [**17, 24, 25, 43**] i.e. dissolving of smaller particles and growth of larger particles. SHI induced reduction in particle size upto fluence of 1×10^{13} ions/cm^2 for the film grown at 200 ºC can be explained either by grain fragmentation [**17, 24, 25, 43**] or by electronic sputtering from the surface of the film [**42**]. The first is due to the generation of strain and the latter owes to transport of mass during impartation of enormous energy by ion beam through the material. The underlying phenomenon can be explicated by Coulomb explosion [**45**] and thermal spike models [**46**]. According to Coulomb explosion model, a highly ionized zone of charged particles is created along the ion trajectory. If target electrons are unable to preserve the charge neutrality on the time-scale of lattice vibration, a quick expansion of the material in the charged domain is produced due to the electrostatic repulsion of ionized target atoms. This quick expansion generates shock waves in the path of ion trajectory. The shock waves so developed in the material cause strain in the grains. Conversely, the thermal spike model predicts that the energy of projectile ion is deposited through the electronic sub-system of the target. This energy is distributed among the electrons by electron–electron coupling and transported consequently to the lattice atoms via electron–lattice interactions, leading to huge increase in the temperature above the melting point of the material, along and in the vicinity of the ion trajectory. The temperature spike builds up pressure waves that cause strain in the grains. The strain so developed leads to fragmentation of grains and consequently, particle size reduces. The above conferred models; Coulomb explosion and spikes refer to the early and late aspects of the ionization track created in a solid by a fast incident ion as proposed by Bringa et al. [**47**]. The extended version of thermal spike postulate explained electronic sputtering from surface in well manner. The flow of mass within the spike becomes relevant at large deposited energies, where the thermal pressure in the hot core of the spike builds up an elastic wave that governs the sputtering yield [**48**]. Though both the phenomena take place simultaneously, the increment in defect density with increase in ion fluence suggests that inside the films, grain fragmentation is taking place whereas on the surface sputtering may be responsible for particle size reduction.

To investigate the role of SHII in creation and annihilation of different energy states responsible for radiative recombination, PL spectra for the films deposited at two different T_s and irradiated at different ion fluences are recorded at room temperature and shown in **Fig. 6 a** and **6 b** respectively. It reveals that both as-deposited films show broad green emission (GE) centered at ~ 2.35 eV and 2.34 eV for films grown at T_s = RT & 200 ºC respectively. The origin of GE at this position is attributed to the transition of sulfur vacancy (V_S) donors to the valence band and conduction band to sulfur interstitial (I_S) [**16, 17, 25, 26**]. The small variation in emission peak position for the pristine films grown at different T_s may be due to difference in crystalline structure. It illustrates from **Fig. 6a** and **b** that the intensity of GE for RT grown pristine film is comparatively larger than that for pristine film grown at T_s=200ºC. This indicates that defect density in the film grown at RT is higher and hence crystallinity is poorer than that for film grown at T_s=200ºC.

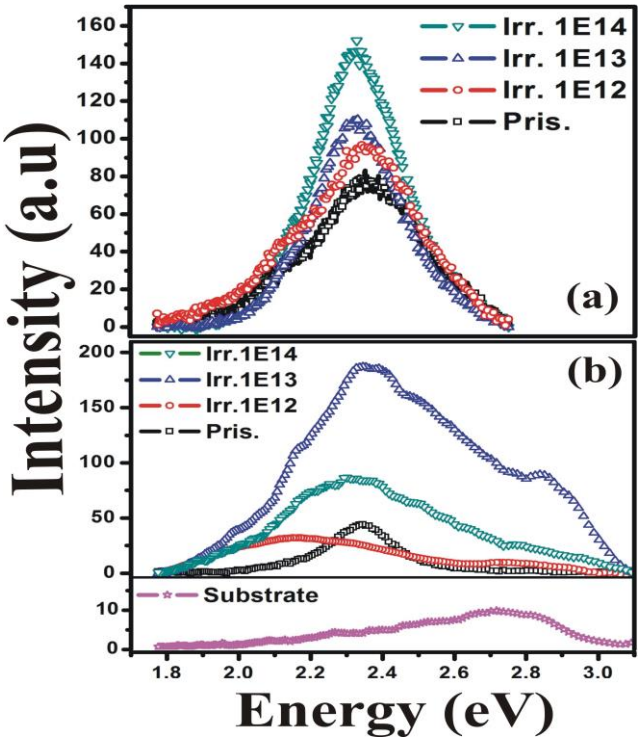

Fig. 6. PL spectra of CdS thin films irradiated at different fluences and grown at (a) RT (b) 200 ºC.

The intensity variation of GE and change in shape of emission spectra with ion irradiation fluence is quite different for the films deposited at two different T_s. It is obvious from **Fig. 6a** that increase in ion fluence causes a slight shift in emission peak towards lower energy side from 2.35 to 2.32 eV with continuous increase in peak intensity with generation of a hump towards lower energy side at ~ 2.15 eV correspond to yellow emission (YE). The YE is originated due to recombination via surface localized states, radiative transition from donor levels i.e. Cd atoms located in interstitial sites (I_{Cd}) to the valence band [**14, 17, 25, 26**] or the transition from interstitial cadmium–cadmium vacancy complexes (I_{Cd}–V_{Cd}) which is a donor to acceptor level transition [**14, 15, 17, 25, 26**]. It seems that the increase in intensity is due to increase in sulfur vacancies after irradiation and shifting towards lower energy side is due to SHI induced generation of defect states like I_{Cd} and/or I_{Cd} –V_{Cd}, which enhances the contribution of YE and results in shifting of spectra peak position. It is observable that the YE hump is disappearing for the film irradiated at 1×10^{14} ions/cm^2 and emission peak becomes sharp with tiny shift towards higher energy. It may

be due to annihilation of defects related to I_{Cd} or $I_{Cd}-V_{Cd}$ at this fluence during recrystallization and phase transition induced by SHII. Recently, the intensity variation, change in shape and shift in emission peak under influence of SHII for the films deposited at T_s=200 ºC has been discussed in detail [**17**]. Previously, we carried out a multi-peak fitting of PL spectra using a Gaussian function for deep analysis of the existence of different emissions related to various defect levels and their contribution in overall emission peak (envelop of emission peaks) as a function of irradiation fluence. The deconvoluted peaks in the experimental data suggested the presence of four peaks lying in the usual range of blue, green, yellow, and orange–red emissions along with substrate peak at ~ 2.77eV. The shift in overall emission peak position was ascribed to shift in the band edge emission due to the quantum confinement effect caused by variation in particle size. The intensity variation and change in shape of spectra was attributed to the variation in population densities of different defect levels contributed to the overall emission and was explained on the bases of GAXRD results. It was noticed from GAXRD scan that at different irradiation fluences either the intensity of some planes was changed or particular planes were disappeared/appeared. This may be due to the electronically activated movement of Cd or/and S atoms from one minimum to the next lower minimum by crossing a potential barrier after SHII. These atomic movements may result in creation/vanish of additional energy states like either I_{Cd}–V_{Cd} and I_{Cd} or I_s–V_s or both during recrystallization under the influence of SHI. Therefore, it may be suggested here that the contribution of particular defect is related to the specific plane [49] and hence strongly dependent on crystalline structure of the film. It is expected that the different behavior of emission spectra shown by the films grown at two different T_s under the influence of SHII is mainly due to the difference in crystalline structure of pristine films.

Conclusion

In summary, the role of growth temperature i.e. T_s to mold the functionality induced by SHII on structural and optical properties of PLDCdS films has been investigated. Here we demonstrated that structural phase transformation into either ZB or WZ is possible by SHII and final phase depends on pre-existing phase which is decided by T_s. The stress developed in the films after SHII is explained on the basis of contributed area of preferred phase in either of the set. It is also shown here that two opposite aspects of SHII i.e. grain growth and grain fragmentation; defect creation and annihilation are not only dependent on ion beam parameter but also on growth temperature induced pre-existing phases. It is illustrated here that the GE observed from the as-deposited CdS thin films becomes intense and broad after SHII in both the cases. However, the shape, broadening and intensity of emission can be controlled by choice of T_s and ion beam parameters collectively. Moreover, the observed broad and intense GE from irradiated samples covers almost full range of visible spectrum which is an excellent feature for photonic applications. SHI induced Ostwald ripening and grain fragmentations are the possible mechanisms for observed enhancement and reduction in particle size respectively.

Acknowledgements

The authors (PK: F.4-2/2006(BSR)/PH/13-14/0055 & NS: F.13-905/2013(BSR)) are thankful to University Grant Commission (UGC), India for providing Dr. D. S. Kothari postdoctoral fellowship. Dr. Ramesh Chandra, Institute Instrumentation Center, Indian Institute Technology (IIT), Roorkee, India is gratefully acknowledged for providing thin film deposition facility. The team work done by the pelletron group, IUAC, New Delhi, India during irradiation experiment are highly appreciable. Authors are heartly thankful to Dr. Fouran Singh for beam time experiment and Raman measurement. The helps received from Dr. Pawan Kulriya IUAC, New Delhi, for GAXRD measurement is highly appreciated. The assistance provided by Mr. Kun Gao, Helmholtz-Zentrum Dresden-Rossendorf, Institute of Ion Beam Physics and Materials Research, Bautzner Landstr, Dresden, Germany during PL measurement is highly acknowledged.

Reference

1. Duan, X.; Huang, Y.; Agarwal, R.; Lieber, C. M. *Nature* **2003**,*421*, 241.
2. Greytak, A. B.; Barrelet, C. J.; Li, Y.; Lieber, C. M. *Appl. Phys. Lett.* **2005**, *87***,** 151103.
3. Grover, R.; Srivastava, R.; Rana, O.; Srivastava, A. K.; Maurya, K. K.; Sood, K. N.; Mehta, D. S.; Kamalasanan, M. N. *J. Luminescence* **2012**, *132***,** 330.
4. Pal, B. N.; Ghosh, Y.; Brovelli, S.; Laocharoensuk, R.; Klimov, V. I.; Hollingsworth, J. A.; Htoon, H. *Nano Lett.* **2012**, *12***,** 331.
5. Sun, F.; Chen, F.; Fei, W.; Sun, L.; Wu, Y., *Sensors and Actuators B.* **2012**, *166***,** 702.
6. Sonawane, N. B.; Ahire, R. R.; Gurav, K. V.; Kim, J. H.; Sankapal, B. R. *J. Alloys and Comp.* **2014**, *592*, 1.
7. Kumar, P.; Kukkar, D.; Deep, A.; Sharma, S. C.; Bharadwaj, L. M.; *Adv. Mat. Lett.* **2012**, *3*, 471.
8. Todorov, T.K.; Gunawan, O.; Gokmen, T.; Mitzi, D. B.; *Progress in Photovoltaics: Res. and Appl.* **2013**, *21*, 82.
9. Balis, N.; Dracopoulos, V.; Bourikas, K.; Lianos, P. *Electrochimica Acta*. **2013**, *91***,** 246.
10. Ullrich, B.; Schroeder, R.; Sakai, H.; Zang, A.; Cheng, S. Z. D. *Appl. Phys. Letts.* **2002**, *80***,** 356.
11. Soundeswaran, S.; Senthilkumar, O.; Ramasamy, P.; Kabiraj, D.; Avasthi, D. K.; Dhanasekaran, R. *Physica B***. 2005,** *355*, 222.
12. Sathyamoorthy, R.; Chandramohan, S.; Sudhagar, P.; Kanjilal, D.; Kabiraj, D.; Asokan, K.*Sol. Energy Mater. Sol. Cells* **2006,** *90*, 2297.
13. Ison, V. V.; Rao, A. R.; Dutta, V.; Kulriya, P. K.; Avasthi, D. K.; Tripathi, S. K. *J. Appl. Phys.* **2009,** *106*, 023508.
14. Lozada-Morales, R.; Zelaya-Angel, O. *Thin Solid Films* **1996,** *281-282*, 386.
15. Vigil, O.; Riech, I.; Garcia-Rocha, M.; Zelaya-Angel, O. *J. Vac. Sci. Tech. A* **1997,** *15*, 2282.
16. Kumar, P.; Saxena, N.; Chandra, R.; Gupta, V.; Agarwal, A.; Kanjilal, D. *Nanoscale Res. Lett.* **2012,** *7***,** 584.
17. Kumar, P.; Saxena, N.; Chandra, R.; Gao, K.; Zhou, S.; Agarwal, A.; Singh, F.; Gupta, V.; Kanjilal, D. *J. Luminescence* **2014,** *147***,** 184.
18. Sakai, H.; Tamaru, T.; Sumomogi, T.; Ezumi, H.; Ullrich, B. *Jpn. J. Appl. Phys.* **1998,** *37*, 4149.
19. Trujillo, O.; Moss, R.; Vuong, K. D.; Lee, D. H.; Noble, R.; Finnigan, D.; Orloff, S.; Tenpas, E.; Park, C.; Fagan, J.; Wang, X. W. *Thin Solid Films* **1996,** *290*, 13.
20. Bilgin, V.; Kose, S.; Atay, F.; Akyuz, I. *Mat.Chem. and Phys.* **2005,** *94*, 103.
21. Tepantlan, C. S.; Gonzalez, A. M. P.; Arreola, I. V. *Rev. Mex. Fis.* **2008,** *54***,** 112.
22. Tong, X. L.; Jiang, D. S.; Li, Y.; Liu, Z. M.; Luo, M. Z. *Physics B* **2006,** *382*, 105; *ibid: Phys. Status Solidi A* **2006,** *203***,** 1992.
23. Saxena, N.; Kumar, P.; Agarwal, A.; Kanjilal, D. *Phys. Status Solidi A* **2012**, *209*, 283.
24. Kumar, M.; Singh, F.; Khan, S. A.; Tripathi, A.; Avasthi, D. K.; Pandey, A. C. *J. Phys. D: Appl. Phys.* **2006,** *39*, 2935; *ibid: J. Luminescence* **2007,** *127*, 302.
25. Chandramohan, S.; Sathyamoorthy, R.; Sudhagar, P.; Kanjilal, D.; Kabiraj, D.; Asokan, K.; Ganesan, V.; Shripathi, T.; Deshpande, U. P. *Appl. Phys. A: Mater. Sci. Process.* **2009,** *94*, 703.
26. Kumar, P.; Saxena, N.; Gupta, V.; Singh, F.; Agarwal, A. *J. Appl. Phys.* **2014,** *116*, 043517.

27. Rizza, G.; Dunlop, A.; Jaskierowicz, G.; Kopcewicz, M. *Nucl. Instrum. Methods Phys. Res. B* **2004,** *226*, 609.
28. Kamarou, A.; Wesch, W.; Wendler, E.; *Phys. Rev. B.* **2008,** *78*, 054111.
29. Mishra, Y. K.; Kabiraj, D; Avasthi, D. K.; Pivin, J. C. *Radiation Effects & Defects in Solids* **2007,** *162*, 207.
30. Saxena, N.; Agarwal, A.; Phase, D. M.; Choudhary, R. J.; Kanjilal, D.; *Physica E* **2010**, *42*, 2190.
31. Chandramohan, S.; Sathyamoorthy, R.; Sudhagar, P.; Kanjilal, D.; Kabiraj, D.; Asokan, K. *Nucl. Instrum. Methods Phys. Res. B* **2007,** *254*, 236.
32. Mochahari, P. K.; Rajbongshi, A.; Choudhury, N.; Singh, F.; Sarma, K.C.; *Adv. Mat. Lett.* **2015**, *6*, 354.
33. www.srim.org
34. Chaudhary, Y. S.; Khan, S. A.; Shrivastav, R.; Satsangi, V. R.; Prakash, S.; Avasthi, D. K.; Dass, S. *Nucl. Instrum. Methods Phys. Res. B* **2004,** *225*, 291
35. Chi, T. T. K.; Gouadec, G.; Colomban, P.; Wang, G.; Mazerollesc, L.; Liem, N. Q. *J. Raman Spectrosc.* **2011,** *42*, 1007.
36. Ghosh, A.; Paul, S.; Raj, S. *Solid state commun.* **2013,** *154*, 25.
37. Balamurugan, B.; Mehta, B. R.; Avasthi, D. K.; Singh, F.; Arora, A. K.; Rajalakshmi, M.; Raghavan, G.; Tyagi, A. K.; Sivaprasad, S. M. *J. Appl. Phys.* **2002,** *92*, 3304.
38. Singh, F.; Kulriya, P. K.; Pivin, J. C. *Solid State Comm.* **2010,** *150*, 1751.
39. Ohring, M.; The Materials Science of Thin films; Academic Press: California: USA, **1992**.
40. Kumar, P.; Saxena, N.; Gupta, V.; Gao, K.; Singh, F.; Agarwal, A. *Adv. Sci. Lett.* **2014,** *20*, 977.
41. Adachi, S.; Properties of Group-IV, III-V and II-VI Semiconductors; John Wiley & Sons: England, **2005**.
42. Singh, F.; Singh, R. G.; Kumar, V.; Khan, S. A.; Pivin, J. C. *J. Appl. Phys.* **2011**, *110*, 083520.
43. Mohanta, D.; Singh, F.; Avasthi, D. K.; Choudhury, A.; *Cent. Eur. J. Phys.* **2006**, *4*, 187.
44. Avasthi, D. K.; Mishra, Y. K.; Singh, F.; Stoquert J. P. *Nucl. Instrum. Methods Phys. Res. B* **2010,** *268*, 3027.
45. Fleischer, R. L.; Price, P. B.; Walker, R. M.; Hubbard, E. L. *Phys. Rev.* **1967,** *156*, 353.
46. Szenes, G.; Horvath, Z. E.; Pecz, B.; Paszti, F.; Toth, L. *Phys. Rev. B.* **2002,** *65*, 045206.
47. Bringa, E. M.; Johnson, R. E. *Phys. Rev. Lett.* **2002,** *88*, 165501.
48. Jakas, M. M.; Bringa, E. M. *Phys. Rev. B* **2000**, *62*, 824.
49. Benyagoub, A. *Phys. Rev. B* **2005,** *72*, 094114.

